MULTIMODAL METHOD IN SLOSHING. PART 2. NONLINEAR MODAL SYSTEMS

ALEXANDER N. TIMOKHA

ABSTRACT. Commonly, two lectures imply a "journey" over necessary background of nonlinear modal modelling in the fluid sloshing problems. Part 1 derives the Lagrange equation, which appears as an infinite-dimensional system of ODE *(modal system)* coupling generalised coordinates and impulses. Here, each generalised coordinate describes a *mode* of surface motions and introducing *natural modes* reforms the Lagrange equations to a *pseudospectral modal system.* Further, to truncate the pseudospectral modal system, we gain an insight into asymptotic steady-state solutions. This makes it possible to establish *the modal ordering*, i.e. relationships between generalised coordinates. Part 2 concerns how to realise the formula:
modal ordering+pseudospectral modal system= multimodal system.
It exemplifies the procedure for 2D and 3D cases and presents some results on nonlinear resonant waves.

1. PRELIMINARIES FROM PART 1

Sketching definitions in Figure 1, let us consider a mobile tank partly filled by an incompressible, inviscid $\boxed{\mathrm{Ga}=\rho^2 L^3 g/\mu^2 \gg 1}$ fluid with irrotational flows. The fluid volume bounded by the free surface $\Sigma(t)$ and the wetted tank surface $S(t)$ is denoted $Q(t)$. Let $O'x'y'z'$ be an absolute coordinate system and $Oxyz$ be a moving coordinate system fixed with respect to the tank. The origin of $Oxyz$ is in the unperturbed free surface and moves with the velocity v_0 relatively to $O'x'y'z'$. The tank has an angular velocity ω relatively to $O'x'y'z'$. The gravity field has

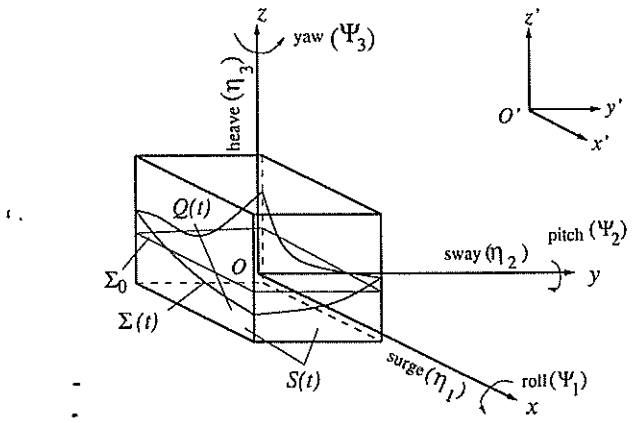

FIGURE 1. Sketch of s smooth tank moving in space. The vectors $\boldsymbol{P}'_O, \omega = (\omega_1, \omega_2, \omega_3)$ and $v_O = (v_{O1}, v_{O2}, v_{O3})$ are considered in the moving coordinate system $Oxyz$ framed with the rigid tank. $Q(t)$ is a piece-smooth, Lipschitzian domain.

the potential $U(x,y,z,t) = -g \cdot r'$; $r' = r'_0 + r$, where r' is the radius–vector of a point of the body–fluid system with respect to O', r'_0 is the radius–vector of the point O with respect to O', r is the radius–vector with respect to O and g is the gravity acceleration vector. Furthermore, v_O and ω are known time-dependent functions, but we should bear in mind that these appear in dynamic equations of the tank as **the unknowns.**

LOGICS OF PART 1:

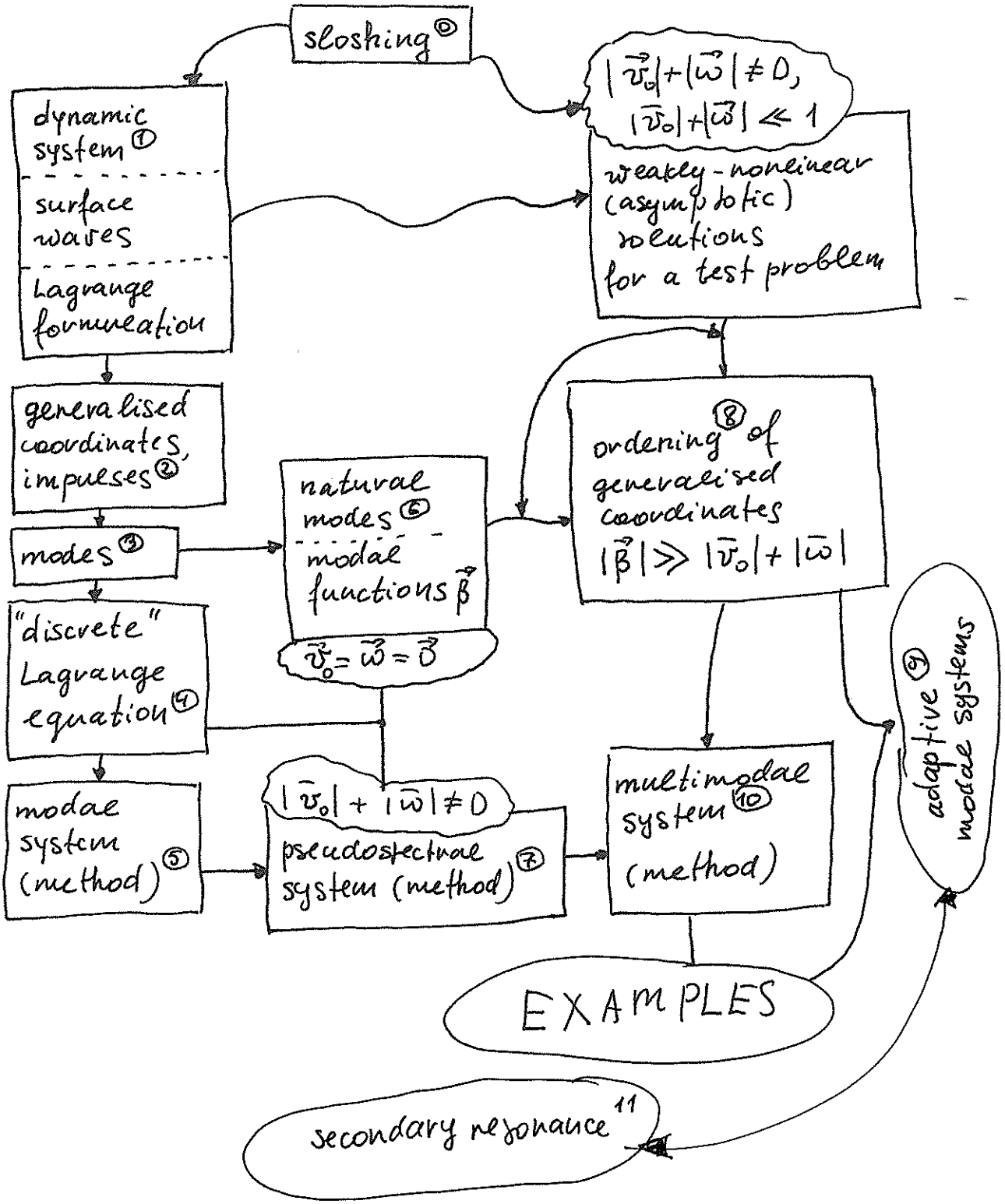

The **first** step of the modal approach consists of introducing the generalised coordinates β_i via the Fourier representation of the free surface $\Sigma(t)$:

$$z = f(x,y,t); \quad f = \sum_{i=1}^{\infty} \beta_i(t) f_i(x,y), \tag{1}$$

where $\{f_i\}$ is a complete system of functions, let's say, a Fourier basis. Each $f_i(x,y)$ determines a wave pattern (profile), a **mode**; (1) is *possible for cylindrical tanks*, more complicated geometry needs special modifications (Lukovsky and Timokha, 2002).

Analogous "Fourier", modal representation for the velocity potential utilises the Kirchhoff solution $K(\beta_i, v_0, \omega)$, which has been found by Zhukovsky for describing the solid body dynamics completely occupied by a fluid (there are no free surface)

$$\Phi(x,y,z,t) = \underbrace{v_0 \cdot r + \omega \cdot \Omega}_{K(\beta_i, v_0, \omega)} + \sum_{k=1}^{\infty} R_k(t) \varphi_k(x,y,z), \tag{2}$$

where $\{\varphi_k\}$ is also a complete system of harmonic functions, $\{R_k\}$ implies the generalised impulses and the Stokes-Zhukovsky potential Ω is solution of Neumann boundary value problem in $Q(t)$.

The **second** step is the derivation of the "discrete" Lagrange equation which couples β, $\boldsymbol{R}$ and follows from a variational principle. The general structure of this equation (associated with Luke-Batemann formulation) is as follows

$$[M(\beta)]\,\dot{\beta} = [F_1(\beta)]\boldsymbol{R} \tag{3}$$

(kinematic part),

$$[M(\beta)]^T \dot{\boldsymbol{R}} = F_2(\beta, \boldsymbol{R}, v_O, \omega, \dot{v}_O, \dot{\omega}) \tag{4}$$

(dynamic part), where $[M(\beta)]$, $[F_1(\beta)]$ and $= F_2(\beta, \boldsymbol{R}, v_O, \omega, \dot{v}_O, \dot{\omega})$ are found in an analytical form as long as f_i and φ_i are also analytical.

The **third** step consists of finding *"natural" modes* f_i and φ_i. The basic idea – the Lagrange equation (3) – (4) should be applicable for modelling small-amplitude (linear) sloshing as $v_O = \omega = 0$. Evaluating the linear sloshing problem describes free-standing surface waves (in the limit $|f| \sim |\nabla\Phi| \to 0$). We obtain a spectral problem on the natural modes. Its solutions are eigenfunctions φ_i and eigenvalues $\kappa_i > 0$, $i = 1, \infty$ determining the surface modes $f_i(x,y) = \varphi_i(x,y,0)$ and natural circular frequencies $\sigma_i = \sqrt{g\kappa_i}$. In some cases, the spectral problem has analytical solutions.

The Lagrange equation (3) – (4) based on the natural modes is called the *pseudospectral modal system.* Generally speaking, the pseudospectral system can be truncated (pseudospectral method) and implemented for direct simulations of nonlinear sloshing. This method works very well for description of nonlinear free-standing waves ($v_O = \omega = 0$), but there are some mathematical, numerical and physical problems, if it is used for simulating resonant sloshing.

Part 1 has finished by considering the **four** step, which should address the question how to operate with *nonlinear forced sloshing.* In order to study this problem analytically, we assume $|v_0| \sim |\omega| \sim \epsilon \ll 1$ and consider the most dangerous situation of lateral (horizontal) harmonic excitations with the forcing frequency σ close to the lowest natural frequency σ_1.

To explain: Why? Ideas?

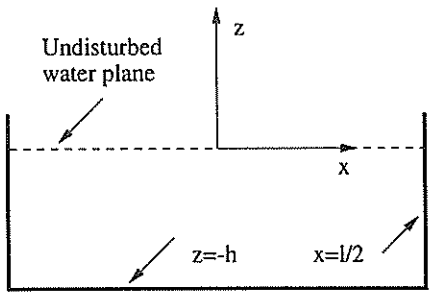

FIGURE 2. Coordinate system.

In many cases, we can find an asymptotic solution of this resonant problem and interpret it in terms of natural modes. Part 2 represents **examples** for 2D and, very shortly, 3D waves.

2. THE MOISEYEV-BASED MODAL SYSTEM FOR A RECTANGULAR TANK

2.1. **Asymptotic periodic solution.** We consider a mobile rectangular rigid tank filled partly by an inviscid incompressible fluid. The **scaled mean water depth** is $h := h/l$ (l is the tank breadth). The origin of the coordinate system lies on the mean free surface, Figure 2. The natural frequencies and modes can be found analytically as

$$\sigma_i = \sqrt{g\pi i \tanh(i\pi h)}, \tag{5}$$

$$f_i(x) = \cos(\pi i(x+1/2)); \quad \varphi_i(x,z) = f_i(x)\frac{\cosh(\pi i(z+h))}{\cosh(\pi i h)}.$$

Evaluating harmonic forcing, for example, $v_0 = (-\epsilon\sigma\sin(\sigma t), 0, 0)$, $\omega = \psi \equiv 0$ as $\epsilon \to 0$, $\sigma \to \sigma_1$, we can find a $2\pi/\sigma$-periodic (steady-state) solution. Faltinsen (1974) did it by using the Moiseyev technique.

Further, this solution can be treated in terms of modes f_i, namely, compared with appropriate Fourier coefficients in

$$f(x,t) = \sum_{i=1}^{\infty} \beta_i(t) f_i(x), \tag{6}$$

$$\Phi(x,0,z,t) = v_{0x}x + v_{0z}z + \omega_2(t)\Omega(x,z,t) + \sum_{n=1}^{\infty} R_n(t)\varphi_n(x,z)$$

(v_{0x} and v_{0z} are projections of translational velocity onto axes of Oxz). This leads to

$$R_1 \sim \beta_1 = O(\epsilon^{1/3}); \quad R_2 \sim \beta_2 = O(\epsilon^{2/3}); \quad R_i \sim \beta_i \le O(\epsilon),\ i \ge 3. \tag{7}$$

The relationship (7) is the required **asymptotic modal ordering**, which must be fulfilled at least for a periodic (steady-state) fluid motions. No warranty that this relationship holds true for arbitrary sloshing, but we *can ASSUME this.*

Derivation: ① resolve (3) relative to R_i ② substitute in (4), terms $O(\epsilon)$

2.2. **Asymptotic modal systems.** Now, for arbitrary motions of the tank (not necessary periodic) with $|v_0| \sim |\omega| = O(\epsilon)$, neglecting $o(\epsilon)$-terms in the pseudospectral system gets the following system of ordinary differential equations

$$(8)\quad (\ddot{\beta}_1 + \sigma_1^2\beta_1) + d_1(\ddot{\beta}_1\beta_2 + \dot{\beta}_1\dot{\beta}_2) + d_2(\ddot{\beta}_1\beta_1^2 + \dot{\beta}_1^2\beta_1) + d_3\ddot{\beta}_2\beta_1 + \\ + P_1(\dot{v}_{0x} - S_1\dot{\omega} - g\psi) + Q_1\dot{v}_{0z}\beta_1 = 0,$$

$$(9)\quad (\ddot{\beta}_2 + \sigma_2^2\beta_2) + d_4\ddot{\beta}_1\beta_1 + d_5\dot{\beta}_1^2 + Q_2\dot{v}_{0z}\beta_2 = 0,$$

$$(10)\quad (\ddot{\beta}_3 + \sigma_3^2\beta_3) + d_6\ddot{\beta}_1\beta_2 + d_7\ddot{\beta}_1\beta_1^2 + d_8\ddot{\beta}_2\beta_1 + d_9\dot{\beta}_1\dot{\beta}_2 + d_{10}\dot{\beta}_1^2\beta_1 + \\ + P_3(\dot{v}_{0x} - S_3\dot{\omega} - g\psi) + Q_3\dot{v}_{0z}\beta_3 = 0.$$

The linear equations describing higher modes are

$$(11)\quad \ddot{\beta}_i + \sigma_i^2\beta_i + P_i(\dot{v}_{0x} - S_i\dot{\omega} - g\psi) + Q_i\dot{v}_{0z}\beta_i = 0, \quad i \geq 4.$$

Here

$$(12)\quad P_{2i-1} = -\frac{8E_{2i-1}}{\pi^2(2i-1)}, \quad P_{2i} = 0; \quad Q_i = 2iE_i, \quad S_i = \frac{2}{\pi i}\tanh(i\pi h/2), \quad i \geq 1.$$

Further,

$$d_1 = 2\frac{E_0}{E_1} + E_1, \quad d_2 = 2E_0\left(-1 + \frac{4E_0}{E_1E_2}\right), \quad d_3 = -2\frac{E_0}{E_2} + E_1,$$

$$d_4 = -4\frac{E_0}{E_1} + 2E_2, \quad d_5 = E_2 - 2\frac{E_0E_2}{E_1^2} - \frac{4E_0}{E_1}, \quad d_6 = 3E_3 - \frac{6E_0}{E_1},$$

$$d_7 = 9E_0 - 12\frac{E_0E_4}{E_1} - 6E_3E_4 + 24\frac{E_0^2}{E_1E_2} + 3\frac{E_0E_3}{E_1}, \quad d_8 = -6\frac{E_0}{E_2} + 3E_3,$$

$$d_9 = -6\frac{E_0}{E_1} - 6\frac{E_0}{E_2} - 6\frac{E_0E_3}{E_1E_2} + 3\frac{E_3E_1}{E_2},$$

$$d_{10} = 18E_0 - 2E_4\frac{12E_0 + 6E_1E_3}{E_1} + \frac{72E_0^2}{E_1E_2} + 12E_0\left(\frac{E_3}{E_1} - \frac{E_1}{E_2}\right),$$

with

$$E_0 = \frac{\pi^2}{8}; \quad E_i = \frac{\pi}{2}\tanh(\pi i h).$$

General structure of these equations is as follows

$$(13)\quad M_1(\beta_1, \beta_2)\ddot{\beta} = F(\beta, \dot{\beta}, t),$$

where $\beta = (\beta_1, \beta_2, \beta_3)^T$ and $M_1 = E$ as $\beta = 0$. The first two nonlinear equations couple β_1 with β_2 and do not depend on β_3. The third mode component is excited by rigid body motions and the first and the second modes.

NB: The nonlinear asymptotic modal systems are characterised by polynomial nonlinearity, where coefficients at the nonlinear terms are only functions of h and can be computed prior to make any simulations.

NB: Even if the asymptotic modal system for sloshing with finite depth has larger dimension, it has the same general structure:

$$(14)\quad M_1(\beta)\ddot{\beta} = F(\beta, \dot{\beta}, t).$$

When $h \to 0$, there is a collision: the matrix $[F_1(\beta)]$ with $\beta = 0$ becomes ill-posed. This disables to resolve (3) with respect to R_i!!!

2.3. **Theory of steady-state motions following from the modal system.** The constructed asymptotic discrete theory (13) makes it possible to generalise some results by Faltinsen (1974). For surge excited steady–state waves we express v_0 as $(-\epsilon\sigma\sin(\sigma t), 0, 0)$, set $\omega = \psi \equiv 0$ and look for periodic solutions

$$\beta_i(t + 2\pi/\sigma) = \beta_i(t), \quad \dot{\beta}_i(t + 2\pi/\sigma) = \dot{\beta}_i(t). \tag{15}$$

To construct the periodic solutions and to derive analytically amplitude–frequency response of nonlinear sloshing in a rectangular tank caused by forced excitation we express the first approximation of the primary mode in the form

$$\beta_1(t) = A\cos\sigma t + o(A), \quad A = O(\epsilon^{1/3}). \tag{16}$$

The substitution of (16) into the modal equation with periodicity condition (15) yields

$$\beta_1 = A\cos\sigma t + o(A); \quad \beta_2 = A^2(l_0 + h_0\cos(2\sigma t)) + o(A^2), \tag{17}$$

where

$$l_0 = \frac{d_4 - d_5}{2\bar{\sigma}_2^2}; \quad h_0 = \frac{d_5 + d_4}{2(\bar{\sigma}_2^2 - 4)}, \quad \bar{\sigma}_i = \frac{\sigma_i}{\sigma}, \quad i = 1, 2. \tag{18}$$

The amplitude $A \sim \epsilon^{1/3}$ must satisfy the equation

$$(\bar{\sigma}_1^2 - 1)A + m_1(\bar{\sigma}_2, h)A^3 - P_1\epsilon = 0, \tag{19}$$

where

$$m_1(\bar{\sigma}_2, h) = d_1(-l_0(\bar{\sigma}_2) + \frac{1}{2}h_0(\bar{\sigma}_2)) - \frac{1}{2}d_2 - 2d_3h_0(\bar{\sigma}_2). \tag{20}$$

The coefficient m_1 in equation (19) depends on the depth/breadth ratio and on σ $(\bar{\sigma}_i, i = 1, 2)$. The last dependence has not been presented earlier for asymptotic solutions, when analogous coefficient in a "secular" equation depends only on h. This means that our asymptotic technique differs from Faltinsen–Moiseev's procedure.

The theory gives the wave amplitude response A of the lowest primary mode versus the excitation period

$$T = \frac{2\pi}{\sigma}$$

coupled by cubic secular equation (19). The response is infinite for $\bar{\sigma}_1 = 1$ and $m_1 = 0$. This means that the third order theory is not valid if

$$m_1(\frac{\sigma_2}{\sigma_1}, h) = 0.$$

The root of the last equation gives $h = 0.3368....$ This is called the critical depth. The response changes from being a 'hard–spring' to a 'soft–spring' at the critical depth.

In our case, $m_1 = m_1(\sigma_2/\sigma, h)$. If a fixed σ is close to the natural frequency σ_1, but $\sigma \neq \sigma_1$ the equation

$$m_1(\frac{\sigma_2}{\sigma}, \bar{h}) = 0 \tag{21}$$

gives a different value of critical depth. This means that the critical depth is a function of σ. If a pair (σ, h) satisfies (21), then A tends to infinity. This effect is illustrated in Figure 3.

Figure 3 shows schematically these theoretical predictions in accordance with theoretical results for 'soft spring'–type response (classification 'soft spring' ('hard spring') solutions is adopted from characteristics of Duffing equation). The first

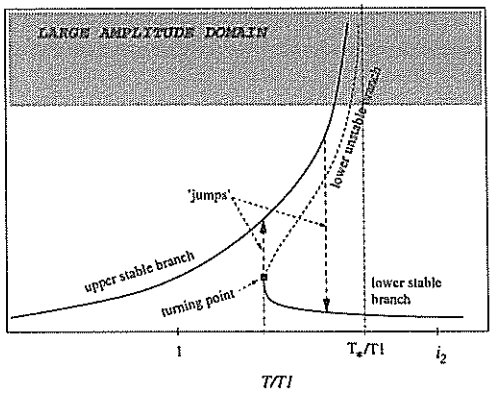

FIGURE 3. The 'soft spring'-type amplitude response in accordance with the modal theory. The fluid depth exceeds the critical value $h = 0.3368....$

FIGURE 4. **Exercise:** The 'hard spring'-type amplitude response in accordance with the modal theory. The fluid depth is less than the critical value $h = 0.3368....$

(upper) branch in Figure 3 implies stable solutions. The second (lower) branch displays stable and unstable steady-state solutions with a turning point between them. The set of turning points for different excitation amplitudes ϵ can be found from the equation $((T/T1)^2 - 1) + 3m_1(h, T/T1)(A)^2 = 0$. The ordinate $T/T1$ of the turning point defines a jump from lower to upper branch. Another jump from upper to lower branch occurs as A increases along upper branch. It occurs for sufficiently large sloshing amplitudes (breakdown is caused by various physical mechanisms including roof impact, viscous damping etc. forcing the sloshing to unsteady regimes) and defines a downshift ('hard spring') or upshift ('soft spring') of maximum wave amplitude response versus $T/T1$ relative to exact linear response $T/T1 = 1$. This pair of jumps puts together the hysteresis between two stable solutions. In accordance with the single dominant model, the maximum downshift (upshift) is always restricted by vertical asymptote $T/T1 = T_*/T1$ found from the

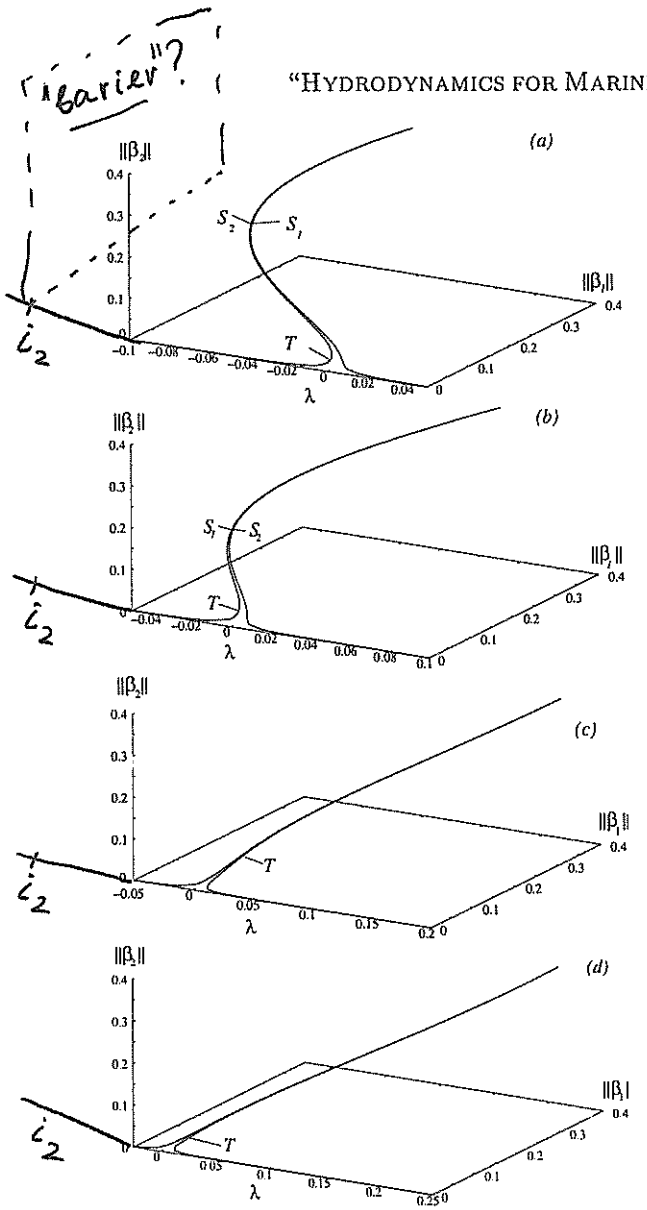

FIGURE 5. Branching for for "Large Amplitude Domain". $\lambda = T1/T - 1$

equation $m_1(h, T_*) = 0$. However, there is no downshift (upshift) for critical fluid depth case, where $m_1(h, 1) = 0$. The third and fifth order single dominant theories give then maximal response for linear resonance $T/T1 = 1$.

Exercise: To draw the response curves for $h < 0.3368...$ in Figure 4.

All the results are based on the assumption that $O(\beta_1^2) = O(\beta_2)$. It may obviously be invalid for transient waves. What about "Large Amplitude Domain"? We used the path-following procedure and found the branching in Figure 5. We see, that the point T_*/T_1 disappears for 'hard spring' response and $O(\beta_1) = O(\beta_2)$!!!

Remark. How to explain that β_2 is the order of the dominating modes? If studying periodic solutions as $\epsilon \to 0$, we can find a critical value of σ/σ_1 for which the amplitude of the second mode tends to infinity. It can happen for small h, or for $\bar{\sigma}_2^2 \to 4$ (see, the asymptotic solution (17) (18)). In terms of σ the condition of the secondary resonance takes the form

$$\frac{\sigma}{\sigma_1} \to \sqrt{\frac{\tanh(2\pi h/l)}{2\tanh(\pi h)}} = i(2,\bar{h}) \to 0, \quad h \to 0. \tag{22}$$

The value $i(2,\bar{h})$ characterises the applicability of the constructed theory. The ratio $T_1/T = \sigma/\sigma_1$ must be close to 1 and not close to $i(2,\bar{h})$. Similarly, we can introduce for the third mode

$$i(3,\bar{h}) = \sqrt{\frac{\tanh(3\pi h/l)}{3\tanh(\pi h)}} \to 0, \quad h \to 0. \tag{23}$$

However since $i(3,\bar{h}) < i(2,\bar{h})$, the secondary resonance is the most dangerous, namely, they appear consequently, beginning with the lower modes, *progressively.* progressive activation of higher modes changes the sloshing from standing to travelling behaviour. Logically, this requires increasing the dimensions.

Thus, the present single dominant theory assumes the excitation amplitude and amplitude response to be very small and gives the tendency of amplitude response with increasing the excitation amplitude. In particular, it shows that the *intersection between the branches increases with excitation amplitude.* For 'soft-spring' (even if $m_1(h,1)$ is very small) this drifts up the turning point to the vertical asymptote $T_*/T1$ in the effective domain of the *secondary resonance* $i_2 = i(2,h)$. Since single dominant theory does not account for secondary resonance, the boundary $T_*/T1$ of the maximal upshift becomes questionable. We can instead use i_2 as boundary of maximal upshift. We expect the effect of the secondary resonance even for the lower fluid depths ('hard spring' response) when amplitudes are sufficiently large. It is then difficult to indicate the downshift (upshift).

Conclusions 1:

1. If external loads on the tank are small with the magnitude $\epsilon \ll 1$, we get an asymptotic modal system (system with only three degrees of the freedom), which captures the dominating resonant $O(\epsilon^{1/3})$-contribution, the second-order terms $O(\epsilon^{2/3})$ and main components of $O(\epsilon)$-contribution. Only the $o(\epsilon)$-order modes are neglected. Even if the forcing is aperiodic, but still with small magnitude, the system will describe not only steady-state regimes, but *also transients on the short-time scale* (Faltinsen et al., 2000).

2. Simulation of *long-time transients* needs accounting for damping. The modal scheme allows for that by computing the damping rates α_i (see Keulegan, 1959) and incorporating them into modal system. This gives

$$M_1(\beta_1,\beta_2)\ddot{\beta} = -2\alpha\dot{\beta} + F(\beta,\dot{\beta},t). \tag{24}$$

Note, that (24) does not include gyroscopic terms and, therefore, the Rayleigh damping α does not lead to instability.

3. Generally speaking, there are three difficulties to implement this modal system.

The first problem is still very small ϵ, but increasing A along the branches. What happen with $A \sim ||\beta_1||$? See Figure 5.

The second problem consists of increasing ϵ.

And, finally, the third problem appears for critical depths $h = 0.3368...$ and shallowing $h \leq 0.2$, where the model is not applicable due to travelling wave phenomena. It is amazing, but all these difficulties are *associated with the secondary resonance phenomena.* These yield *MULTIPLE-dominating, ADAPTIVE system* with

$$\beta_1 \sim \beta_i = O(\epsilon^{1/3}), \quad i = 2, N. \tag{25}$$

How large should be N? In order to address this question, we should consider embedding modal systems so that structure of each a consequently new system follows from failure of the earlier one.

FOR NOTES:

3. Adaptive modal scheme with non-infinitesimal ϵ

Point 1. The position of secondary resonance does not depend on excitation amplitude. The asymptotic theory ($\epsilon \to 0$) does not give the value of effective domain for primary and secondary resonance. For sufficiently small ϵ the effective domains do not overlap with each others. But the overlapping can happen with increasing ϵ and A. In addition, the effective domains can get a downshift or upshift. It also leads to overlapping with these domains. Two or more modes having the same order are then involved in resonant sloshing.

Point 2. The Lagrange equation has general multidimensional structure, which can be adopted for multimodal resonant excitation. It requires preliminary analysis to start the simulation of steady-state solutions. The analysis is connected with an 'a priori' prediction of inter-modal resonances. In simplified form it can be treated as the following adaptive procedure. We consider a series of natural frequencies $\sigma_1, \sigma_2, \sigma_3, ...$ and a set of possible frequencies $\sigma, 2\sigma, 3\sigma, ...$ caused by main excitation frequency σ. If main frequency σ is close to one of the natural frequencies of odd modes and away from other modes, this mode is primary excited. In order to add the most dangerous secondary resonance we should find the mode (even or odd) of which the natural frequency is close to 2σ. Reconstruction of the effective domains (based on condition $||\beta_1|| = ||\beta_2||$) done by a path-following procedure along the response curves is given in Figure 6.

Point 3 (example by Faltinsen and Timokha (2001)). Let us assume as an example that these two modes correspond to β_1 and β_2. The two first nonlinear equations of general system give a kernel of this interaction. Any other mode β_m can be considered as having lower order or driven (they are linear in β_m and nonlinear in dominating modes). The secondary resonance implies $\beta_2 \sim \beta_1$. This means, that additional nonlinear terms in β_1 and β_2 should be included. Two of the equations take then the following form

$$\ddot{\beta}_1(1+D1^1(1,2)\beta_2+D2^1(1,1,1)\beta_1^2+D2^1(1,2,2)\beta_2^2)+\ddot{\beta}_2(D1^1(2,1)\beta_1+D2^1(2,2,1)\beta_2\beta_1)+$$
$$+T0^1(1,1,1)\dot{\beta}_1\dot{\beta}_1\beta_1+T1^1(2,2,1)\dot{\beta}_2\dot{\beta}_2\beta_1+\dot{\beta}_1\dot{\beta}_2(T0^1(2,1)+T1^1(2,1,2)\beta_2)+$$
$$+\sigma_1^2\beta_1+P_1(\dot{v}_{0x}-g\psi)+\dot{\omega}Q_1L_1^{(0)}=0,$$
$$\ddot{\beta}_1(D1^2(1,1)\beta_1+D2^2(1,2,1)\beta_1\beta_2)+\ddot{\beta}_2(1+D2^2(2,1,1)\beta_1^2+D2^2(2,2,2)\beta_2^2)+$$
$$+\dot{\beta}_1\dot{\beta}_1(T0^2(1,1)+T1^2(1,1,2))+T1^2(2,2,2)\dot{\beta}_2\dot{\beta}_2\beta_2+T1^2(2,1,1)\dot{\beta}_1\dot{\beta}_2\beta_1+\sigma_2^2\beta_2=0, \quad (26)$$

where $D1, D2, T0$ and $T1$ are explicitly give functions of h (Faltinsen and Timokha, 2001).

This system is of third polynomial order in β_1 and β_2. It contains all the necessary terms of Faltinsen–Moiseyev theory and a theory considering $\beta_1 \sim \beta_2 = O(\epsilon^{1/2})$. In addition, the third order terms similar to $\beta_2^3, \beta_2^2\beta_1$ are included to describe a "switch" between these asymptotics during transients when $\beta_1 \sim \beta_2 = O(\epsilon^{1/3})$ in framework of a third order theory. The responses of third and fourth modes are not included in the presented equations. They can be considered as driven. Four equations for $\beta_3, \beta_4, \beta_5$ and β_6 are nonlinear in β_1 and β_2 and linear in $\beta_3, \beta_4, \beta_5$ and β_6 respectively.

When the three modes β_1, β_2 and β_3 have the same order, the corresponding nonlinear system of differential equation can be derived in a similar way. It couples three modal functions up to terms of third order. A similar procedure can also be made for primary excited non–lowest natural mode.

Even if we derived (26) adapted to describe steady-state solutions, it can be used for simulation of beating waves. These waves appear in initial phase due to nonlinear interaction between natural and forced solutions.

Point 4 (general adaptive scheme). Modal functions in general case can be associated with an order $\beta_i = O(\epsilon^{p_i/K})$, where K is the order of the theory and

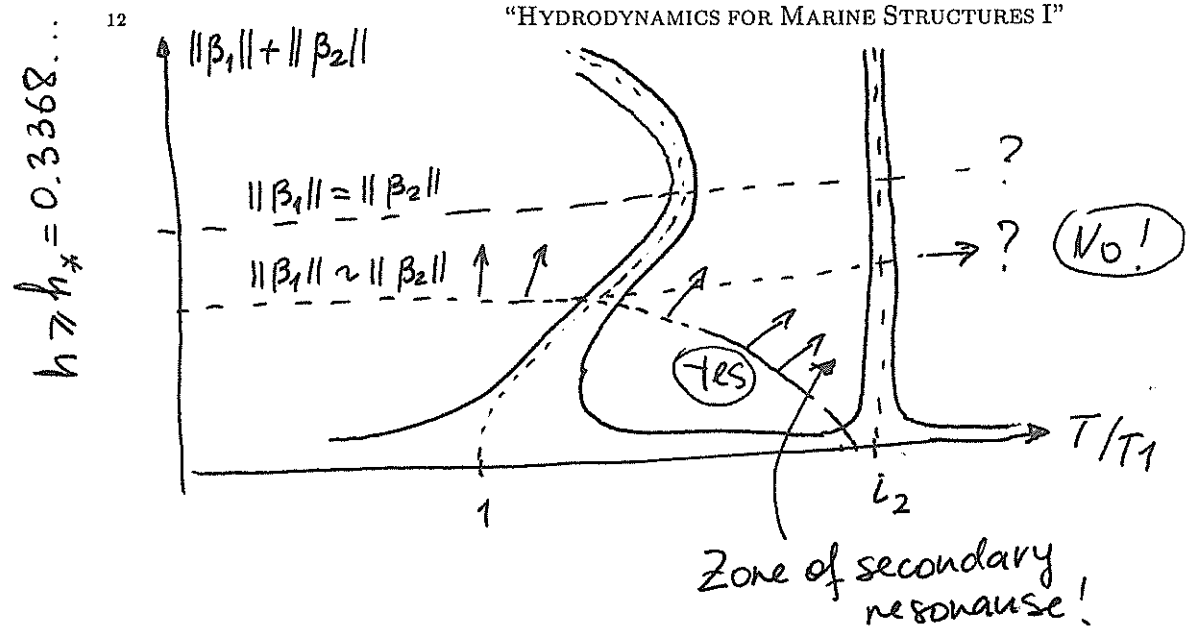

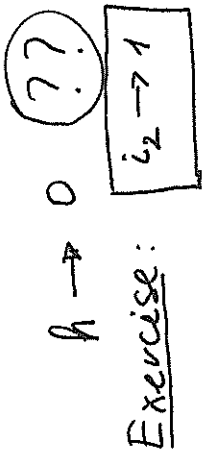

FIGURE 6. Effect of the effective domain of the secondary resonance. Reconstruction is based on the path-following analysis.

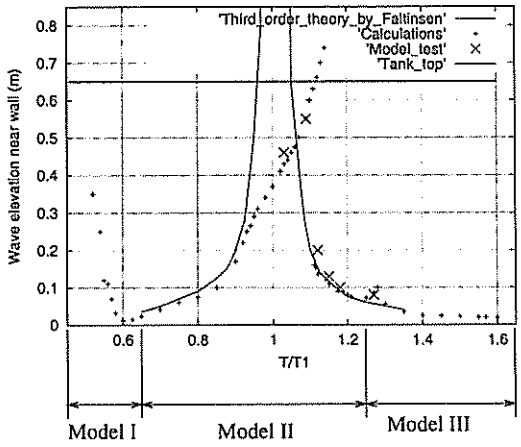

FIGURE 7. Wave elevation near the wall vs "period–first natural period ratio", $h = 0.35, \epsilon = 0.025$.

$p_i \leq K$. The analytical conditions in summations should couple p_i instead of indexes i. In order to keep only terms of $O(\epsilon)$ we use the condition $\sum p_i \leq K$. For example, $\sum_{a,b,c,d=1}^{\infty}$ should be accompanied by condition $p_a + p_b + p_c + p_d \leq K$. These conditions allow us to avoid analytical manipulations to derive particular cases of uniformly valid system detuned for different sets of p_i.

Point 5 (examples). Physically-based calculation strategy of steady-state solutions may be based on solving the initial Cauchy problem for adaptive modal system. A very small linear damping term $2\alpha\sigma_i\dot{\beta}_i$ is incorporated into each ith modal equation, where α was varied from 0.005 to $10^{-6} - 10^{-7}$. The long time series will therefore give an approximation of steady-state solutions due to damping effects. Our estimates of the damping is based on the theory by Keulegan (1959) (maximal value $\alpha \approx 0.005$ is consistent with his prediction for the primary mode). The time integration started normally from zero initial conditions unless we expect two steady-state solutions in the hysteresis domain. The time integration procedure was then continued with initial conditions obtained from previous simulation. This makes it possible to follow the branches by our computational scheme and, therefore, describe the hysteresis. Some discussions on that is given below. The maximum damping coefficient was used for first time series. When the numerical solution gets a periodic structure, the damping coefficient was decreased by a factor of 10. The time to reach this periodical solution increases exponentially with decreasing α. This limits us to use uniformly smaller α. Only some isolated cases near turning points predictions were tested with $\alpha = 10^{-8} - 10^{-10}$.

Surge excited resonant sloshing in a rectangular tank with mean fluid depth close to critical value $h = 0.3368$ was studied experimentally. Steady–state fluid response was compared with the third order Moiseyev's theory. This theory predicts infinite response as $T \to T1$ at the critical depth. If the higher order Moiseyev–like theory is used, the response will be finite. But the predicted amplitudes are much larger and unrealistic relative to the experiments for the fluid depth/tank breadth ratio $h = 0.35$ presented in Figure 7. When decreasing these coefficients even small numerical error leads to a new series of large amplitude transients. This means

Do read at home!

hydrodynamic instability instead of stable sloshing found in experiments. Since the response of higher modes becomes of the same order as primary mode, it also means that secondary resonance effective domain overlaps with the lowest mode resonance zone. We have therefore applied an adaptive method to this problem.

The numerical results by our calculation method are shown in Figure 7. The calculation procedure has some stages. The first stage of the analysis was to locate four possible resonances for $T/T1$ between 0.45 and 1.65. The primary resonances of the first and third mode occur at respectively $T/T1 = 1$ and $T/T1 = 0.55$. The secondary resonance of the second mode is predicted at $T/T1 = 1.28$. The secondary resonance of the third mode is at $T/T1 = 1.55$. Three models applicable for different period domains were used. They are indicated as Model I, II and III (it was controlled that the models overlap with each other in a small domain). Model I was used for $0.5 \leq T/T1 \leq 0.65$. The expected resonances are due to primary excitation of the third and first mode. They have the same main frequency response σ. No secondary resonance is expected. This causes the relations $\beta_1 \sim \beta_3 = O(\epsilon^{1/3})$. This means that the secondary modes have the main harmonic 2σ. Such modes are $\beta_2 \sim \beta_6 = O(\epsilon^{2/3})$. Other modes (up to 9th) are considered as driven and having $O(\epsilon)$. The modal system based on (26) (Model II) was used for $0.6 \leq T/T1 \leq 1.28$. The modes $\beta_3, \beta_4, \beta_5, \beta_6$ were included as driven. If response is not too large, the modal system (26) gives the same results as shown by third order response by Faltinsen (1974)). When $T/T1 > 1.28$, the third mode response was assumed to have the same order as β_1 and β_2 (Model III). The reason is the influence of the secondary resonance of third mode at $T/T1 = 1.55$. Model III was used for $1.28 < T/T1 < 1.65$.

The calculations accounting for secondary resonances are in good agreement with experiments. It improves the single dominant theoretical prediction between $0.9 < T/T1 < 1.11$ (primary resonance) and $1.21 < T/T1 < 1.32$ (secondary resonance of the second mode). In accordance with our calculations the maximum response is situated at $T/T1 = 1.11$ instead of preliminary prediction $T/T1 = 1$. This gives the upshift of the maximum amplitude response in good agreement with experimental data. A local maximum is experimentally and numerically found at $T/T1 = 1.3$. This maximum response is caused by secondary resonance phenomenon. Note, that the computation strategy allows to follow along upper branch up to very large amplitudes in the cases $T/T1 = 1.11$ and $T/T1 = 1.3$ when using the results of previous calculations as initial Cauchy conditions in new time series. Only numerical instability and the involvement of many secondary modes in resonance stop us to continue the branch to infinity. For the case in Figure 7 (Model II) these difficulties appear as wave amplitude tends to $1m$ corresponding to $T/T1 = 1.21$. On the other hand, we cannot follow leftwards of $T/T1 = 1.11$ along the lower branch. The turning point limits us from doing this. The simulations give then a series of transients resulting in the stable steady solution on the upper branch. This means we cannot avoid a hysteresis effect occurring around $T/T1 = 1.11$ and $T/T1 = 1.3$ in the simulations. The period increment in the experiment were probably too large to detect this hysteresis. In addition, the transient wave amplitudes will in reality cause a series of heavy roof impacts, which damp the system and eliminate large amplitude steady-state waves for excitation periods higher than $T/T1 = 1.11$. The presented model does not account for roof impact.

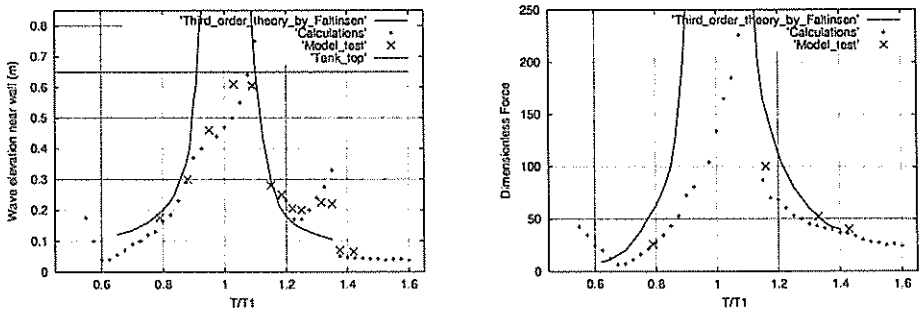

FIGURE 8. Wave elevation near the wall and dimensionless lateral force $1000F_x/(\rho g l^2 b)$ vs "period–first natural period ratio", $h = 0.35, \epsilon = 0.05$.

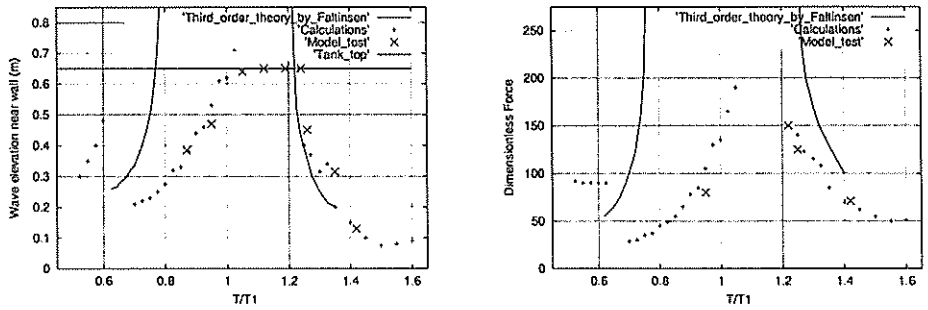

FIGURE 9. Wave elevation near the wall and dimensionless lateral force $1000F_x/(\rho g l^2 b)$ vs "period–first natural period ratio", $h = 0.35, \epsilon = 0.1$.

Since the excitation amplitude is small in the case of Figure 7, the local maximum at secondary resonance $T/T1 = 1.3$ is not too large. However, it increases with excitation amplitude H. Figures 8 and 9 present comparisons between experiments and calculations for larger excitation amplitudes. The tank and fluid depth is the same as used for Figure 7. Both wave elevation near the tank wall and lateral fluid force are examined. (The symbol b used in expression for dimensionless force means the tank length.) The simulation strategy in using Models I, II and III did not change. Out calculations show that the effective domain of secondary resonance increases with increasing excitation amplitude. It covers the range from 0.6 to 1.28 in Figure 9. The jump in wave elevation response also increases at $T/T1 = 1.3$. The experiments and our calculations show that the increasing of the amplitude in Figures 7 and 8 give small change of the upshift caused by main resonance, but sufficient upshift near secondary resonance. The both upshifts becomes larger with increasing amplitude in the case of Figure 9.

The effective domain of the secondary resonance by the third mode also increases. Since only odd modes contribute to the lateral force, the secondary resonance of the second mode is generally more important for wave elevation than for lateral force. However, for sufficiently large excitation amplitude the effect of secondary resonance becomes also important for lateral force. The reason is the inter-modal

I do read at home

interaction between nearest odd modes β_1 and β_3 which due to secondary resonance of the third mode interact nonlinearly with each other and have the same order.

Conclusions: (to be formulated together with lecturer)

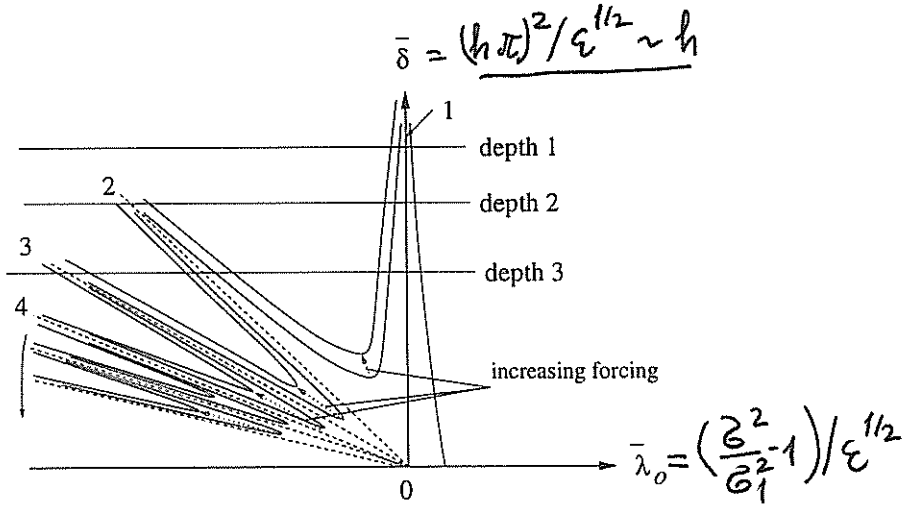

FIGURE 10. Schematic picture of possible secondary resonances in the detuning/depth $(\bar{\lambda}_O, \bar{\delta})$ plane. Here the numbers of the 'fingers' correspond to various modes amplification: 1 (near the line $\bar{\lambda}_O = 0$) implies the primary resonance, 2 (near the line $\bar{\delta} = -\bar{\lambda}_O$) corresponds to the secondary resonance of the second mode, 3 (near the line $\bar{\delta} = -\frac{3}{8}\bar{\lambda}_O$) corresponds to the secondary resonance of the third mode and so on. Number of intersections increases with increasing forcing amplitude.

4. PASSAGE TO SMALL DEPTH

Details: Shallow fluid sloshing has been extensively studied by various authors. For example, (Chester, 1968) derived for this case a viscous and dissipative theory agreeing with experiments by (Chester and Bones, 1968). A unique modal theory of sloshing for small depths in given by Faltinsen and Timokha (2002).

Since $i_n \to 1$ as $h \to 0$, the secondary resonance becomes of primary importance to explain passage to shallow fluid sloshing. Accounting for this limit gives the best classification of the nonlinear sloshing as a function of the depth (dispersive features of the linear sloshing). When the fluid depth is not small, the natural frequencies σ_i complete a non-commensurate spectrum, such that $\sigma_i \not\approx i\sigma_1$. The undamped steady-state resonance is then according to Faltinsen and Timokha (2001) analogous to the the single or coupled Duffing oscillators. However the response for shallow depth is quite different when any of the natural frequencies are commensurate, or, due to small dispersion, nearly commensurate ($i_n \approx 1$ for all or at least a large number of modes). This activates them progressively due to secondary resonances and may result in shock waves (bores). Faltinsen and Timokha (2001, 2002) discussed the details of this mechanism in order to match with finite fluid depth theories. They showed that under certain circumstances the adaptive models may describe resonant sloshing only for $0.24 \lesssim h$. The intermediate depths $0.1 \lesssim h \lesssim 0.24$ require a special asymptotics accounting for smallness of h. Corresponding modal system must by using the language of modal decomposition include terms up to $O(\epsilon)$ within relationships

$$R_i \sim \beta_i \sim h^* = O(h^*) = O(\epsilon^{1/4}). \tag{27}$$

The asymptotic modal system emerging from (27) was derived by Faltinsen and Timokha (2002) to account for smallness h, keep the quantities of the adaptive modal system by

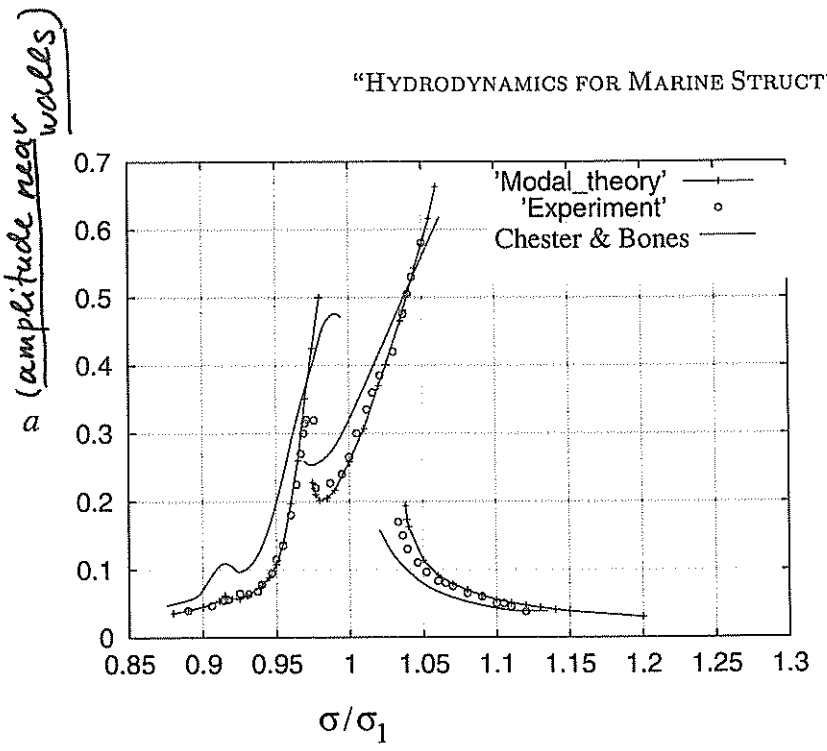

FIGURE 11. Dimensionless wave elevation near the vertical wall proposed for shallow fluid ($a = (f_{max} - f_{min})/h$ vs excitation σ/σ_1). Rectangular tank with $h = 0.08333, \epsilon = 0.001254$. H is the surge (sway) excitation amplitude. The calculated data are for water with $\nu = 1.1 \cdot 10^{-6}[m^2/s]$. 'Modal theory' present results by Faltinsen and Timokha (2002), 'Experiment' denotes the measurements by Chester and Bones (1968) and 'Chester & Bones' means results by the second order shallow water theory by Chester (1968).

Faltinsen and Timokha (2001) and, with decreasing h include all the necessary second order terms required by Ockendon's asymptotics. By surveying appropriate asymptotics of shallow fluid sloshing we found that (27) implies a modified Boussinesq model. Faltinsen and Timokha (2002) showed that (27) yields the Padé-approximant of the natural spectrum. Now, the analysis becomes a lot clearer and the region in the excitation frequency/depth plane, where the secondary resonances are expected, may be asymptotically estimated by following the general scheme developed for an acoustic resonator. A descriptive comparison can be done by introducing the Moiseyev detuning λ_O ($\bar{\lambda}_O$) i.e. $\sigma^2 = \sigma_1^2(\lambda_O + 1)$ and relating this as $O(\epsilon^{1/2}) = \lambda_O = \epsilon^{1/2}\bar{\lambda}_O$. Further, we should introduce $\delta = (h\pi)^2 = \bar{\delta}\epsilon^{1/2}$ characterising the dimensionless depth. The resonant regions are in accordance with shallow fluid sloshing prediction associated with $\bar{\lambda}_O$ and $\bar{\delta}$, where $|\lambda_n| = |-n^2\epsilon^{1/2}(\bar{\lambda}_O + \bar{\delta}\frac{1}{3}(n^2-1)) + O(\epsilon)| \ll O(\epsilon^{1/2})$, $n \geq 1$. This occurs in a vicinity of the solutions $\bar{\lambda}_0 = 0$, $n = 1$ (the primary resonance) and $\bar{\lambda}_O + \bar{\delta}\frac{1}{3}(n^2-1) = 0$, $n \geq 2$ (the secondary resonances). Those regions are in the $(\bar{\lambda}_O, \bar{\delta})$ (detuning/depth) plane confined to narrow 'fingers', each of which corresponds to Duffing-like superharmonic resonance. They are schematically shown in figure 10. The 'fingers' can dramatically be 'rounded off' by dissipation. This is of primary importance for higher modes. However, number of intersections with 'fingers' growths with the forcing. This clarifies why the large amplitude forcing may lead to the secondary resonance by a few of lowest modes even if the fluid depth is not small enough. In order to interpret the qualitative theory, we intersected the

'fingers' by horizontal lines implying different fluid depths. First of all we should note, that intersections with 'fingers' are expected near the main resonance (finger 1) and for negative $\bar{\lambda}_O$ ($\sigma/\sigma_1 < 1$). For larger depths, we can see, that the line will not cross the region of possible shock waves (due to 'round off'), or, at least will cross it away of the main resonance, namely with sufficiently large negative detuning $\bar{\lambda}_O$. The number of possible intersections may dramatically increase with decreasing $\bar{\delta}$ (depth) and increasing forcing amplitude. The number of solutions for any fixed excitation frequency (detuning) increases as $h \to 0$ and it is expected possible jumps from one to another. Since the dissipation increases with mode number, it should 'round off' first of all 'fingers' with large numbers in figure 10 and connect the solutions in a bounded response. When excitation amplitude is sufficiently small, the damping is mainly caused by viscous dissipation in boundary layers at the tank surface. A classical example with corresponding experimental measurements was presented by Chester and Bones (1968). Starting from the secondary resonance concept Faltinsen and Timokha (2002) derived a Boussinesq-like dissipative theory to handle intermediate and shallow sloshing where dissipation may matter. It showed high level of applicability. An example is presented in figure 11. Here the mean depth $h = 0.08333$ and amplitude $\epsilon = 0.00077874$[m] ($\epsilon/h = 0.0155$). The results in figure 11 agree well with the experiments. It gives clearly better theoretical results than presented by Chester and Bones (1968).

Conclusions and problems: (to be formulated together with lecturer)

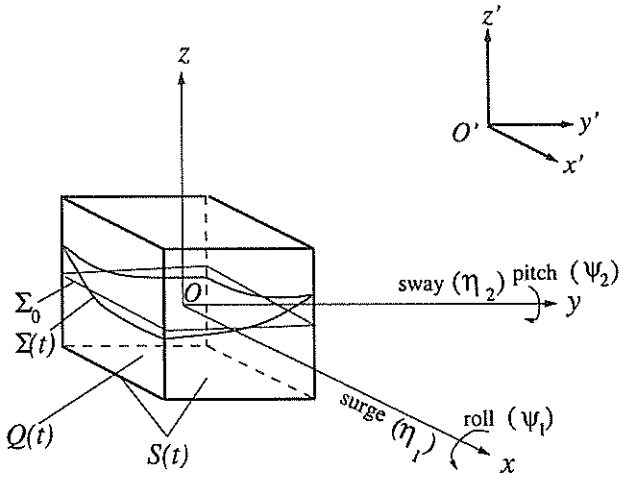

FIGURE 12. Sketch of a square base tank forced in sway/surge and roll/pitch. The vectors $\omega = (\omega_1, \omega_2, 0)$ and $v_O = (v_{O1}, v_{O2}, 0)$ are considered in the moving coordinate system $Oxyz$ framed with the rigid tank.

5. EXAMPLES ON THREE-DIMENSIONAL SLOSHING. MOISEYEV-SCHEME FOR SLOSHING IN A (NEARLY) SQUARE BASE TANK

Let a square base tank with the base breadth L_1 be partially filled by a perfect fluid with the mean depth h. We assume potential flow and make lengths non-dimensional by dividing with L_1, so that tank's breadth and width are equal to 1. A consequence is that values of the physical parameters including $h := h/L_1$ and $g := g/L_1$ (g is the gravity acceleration) are re-defined so that h in the following text is dimensionless while g has dimension $[s^{-2}]$. Combined prescribed sway/surge and roll/pitch motions of the tank are described by a pair of time-dependent vectors $v_O(t) = (v_{O1}(t), v_{O2}(t), 0)$ and $\dot{\psi}(t) = \omega(t) = (\omega_1(t), \omega_2(t), 0)$ representing instantaneous translatory and angular velocities of the mobile Cartesian coordinate system $Oxyz$ relative to an absolute coordinate system $O'x'y'z'$ (Figure 12). The coordinate system $Oxyz$ is rigidly framed with the tank. Its origin O coincides with the middle point of the mean fluid surface which belongs to the Oxy-plane so that the Ox and Oy-axes are parallel to the vertical walls. When $v_O = \omega = \mathbf{0}$ the linear sloshing problem has the fundamental solutions $\Phi = \exp(I\sigma_{i,j}t)\varphi_{i,j}(x,y,z)$, $(I^2 = -1)$, where the natural modes (complex amplitudes) $\varphi_{i,j}$ are computed by

$$
\begin{aligned}
&\varphi_{i,j}(x,y,z) = f_{i,j}(x,y)\frac{\cosh(\lambda_{i,j}(z+h))}{\cosh(\lambda_{i,j}h)},\\
&f_{i,j}(x,y) = \cos(\pi i(x-\frac{1}{2}))\cos(\pi j(y-\frac{1}{2})),\\
&\lambda_{i,j} = \pi\sqrt{i^2+j^2},\quad \sigma_{i,j}^2 = g\lambda_{i,j}\tanh(\lambda_{i,j}h),\quad i,j \geq 0,\quad i+j \neq 0
\end{aligned}
\tag{28}
$$

and $\sigma_{i,j}$ are the natural circular frequencies. Projections of $\varphi_{i,j}$ on the mean free surface $z = 0$ define shapes of standing waves $\{f_{i,j}(x,y) = \varphi_{i,j}|_{z=0},\ i+j \geq 1\}$ that constitute an appropriate Fourier basis in the square cross-section of the tank. The functions $\{\varphi_{i,j}(x,y,z),\ i+j \geq 1\}$ form a complete system of harmonic functions in

the unperturbed fluid domain $Q_0 = [-1/2, 1/2] \times [-1/2, 1/2] \times [-h, 0]$, which satisfies zero-Neumann boundary conditions on the tank surface. The modal technique suggest the free surface elevation $z = f(x, y, t)$ to be presented in the tank-fixed $Oxyz$-coordinate system as

$$f(x, y, t) = \sum_{i+j \geq 1}^{\infty} \beta_{i,j}(t) f_{i,j}(x, y), \tag{29}$$

where $\{f_{i,j}(x, y),\ i + j \geq 1\}$ are natural surface modes and the unknown time dependent modal functions $\beta_{i,j}(t)$ are either computed analytically via an asymptotic procedure or, via substituting (29) into the original non-dimensional free boundary problem, found from a multidimensional system of ordinary differential equations (modal system). The modal modelling using truncated series (29) implies also some additional limitations on instantaneous surface shapes including requirements of right contact angles at the vertical walls and no wave breaking, but the modal technique makes it possible to account for damping and, in its multidimensional form, for amplification of higher modes.

Let us assume that the external forcing is a harmonic function of time as follows $\dot{v}_{Oi} = -\sigma^2 \epsilon_i \cos \sigma t$ and $\dot{\omega}_i = -\sigma^2 \varepsilon_{0i} 2\pi \cos \sigma t,\ i = 1, 2$ with

$$\epsilon_1 = \epsilon \cos\theta,\quad \epsilon_2 = \epsilon \sin\theta;\quad \varepsilon_{01} = \varepsilon \cos\theta,\quad \varepsilon_{02} = \varepsilon \sin\theta \tag{30}$$

($\epsilon \ll 1$ is the non-dimensional amplitude of translatory excitation, ε is the non-dimensional angular amplitude and $(\cos\theta, \sin\theta)$ is the guiding vector of the excitations). The resulting non-dimensional amplitude for the combined horizontal and angular excitations can be defined as

$$\delta = \sqrt{\epsilon^2 + \varepsilon^2}. \tag{31}$$

Using the modal technique based on the representation (29) and the third-order Moiseyev ordering

$$\beta_{i,j} = O(\delta^{1/3}),\ i + j = 1;\quad \beta_{i,j} = O(\delta^{2/3}),\ i + j = 2;\quad \beta_{i,j} \leq O(\delta),\ 3 \leq i + j \tag{32}$$

Faltinsen *et al.*Faltinsen et al. (2003); ? classified the asymptotic periodic solutions (in the asymptotic limits $\delta \to 0$) which has been derived up to third-order terms $O(\delta)$. Although these solutions can be obtained by either direct expansions by $\delta^{1/3}$ in the original free boundary value problem, a five-dimensional nonlinear modal system coupling $\beta_{i,j},\ i+j \leq 3$ of (32), which may describe related transient sloshing and wave motions with non-harmonic forcing, was also derived. The lowest-order terms of these asymptotic solutions are

$$\begin{aligned} &\beta_{1,0}(t) = A \cos \sigma t + \bar{A} \sin \sigma t + O(\delta);\quad \beta_{0,1}(t) = \bar{B} \cos \sigma t + B \sin \sigma t + O(\delta), \\ &\beta_{i,j}(t) = O(\delta^{i/3}),\ i + j = 2, 3;\quad \beta_{i,j}(t) = o(\epsilon),\ i + j \geq 4 \end{aligned} \tag{33}$$

where $A, \bar{A}, B, \bar{B} = O(\delta^{1/3})$. The dominating amplitudes $A, \bar{A}, B, \bar{B}$ are governed by a system of nonlinear algebraic equations, which does not always have a solution and may have multiple solutions.

The case of longitudinal forcing ($\varepsilon_2 = \epsilon_2 = 0$ or $\theta = 0$) is characterised by three and only three types asymptotic solutions (33) that take the following form:
(i) 'planar'

$$f(x, y, t) = A f_{1,0}(x) \cos \sigma t + o(\delta^{1/3}), \tag{34}$$

occurring when $A \neq 0$ and $\bar{A} = B = \bar{B} = 0$ (solution implies two-dimensional sloshing in the plane of excitation),
(ii) 'squares'-like

$$f(x,y,t) = \left[A f_{1,0}(x) \pm \bar{B} f_{0,1}(y)\right] \cos \sigma t + o(\delta^{1/3}) \tag{35}$$

occurring for $A \neq 0$ and $\bar{A} = B = 0$, $\bar{B} \neq 0$ (here, $|A| \neq |B|$ and (35) corresponds to a nearly diagonal standing wave, but $\pm$ implies the possibility that the waves can occur approximately along either of the two diagonals), and, finally,
(iii) 'swirling'

$$f(x,y,t) = A f_{1,0}(x) \cos \sigma t \pm B f_{0,1}(y) \sin \sigma t + o(\delta^{1/3}) \tag{36}$$

occurring for $A \neq 0$ and $B \neq 0, \bar{B} = \bar{A} = 0$. The reason why (36) describes 'swirling' is that the x and y-dependent terms are 90^0 out of phase. The $\pm$ ahead of amplitude component B in (36) means clockwise or counterclockwise rotary waves. Initial conditions and transient phase will determine the sign. Because of both signs possible in (35) (36), (i-iii) implies not three, but five different solutions.

The case of diagonal excitations leads to the same 'squares'-like sloshing, but
(i*) 'diagonal' wave regime

$$f(x,y,t) = A\left[f_{1,0}(x) \pm f_{0,1}(y)\right] \cos \sigma t + o(\delta^{1/3}) \tag{37}$$

($\pm$ for $\theta = \pi/4$ or $3\pi/4$ in (30), respectively) occurs instead of the 'planar' (i) and another structure have
(iii*) 'swirling', i.e.

$$f(x,y,t) = (A \cos \sigma t \pm B \sin \sigma t) f_{1,0}(x) + (A \cos \sigma t \mp B \sin \sigma t) f_{0,1}(y) + o(\delta^{1/3}) \tag{38}$$

with $|A| \neq |B|$ $A \neq 0$, $B \neq 0$. Although (38) also determines a swirling and the sign in (38) depends on initial conditions, it is not equivalent to (36). One obvious fact is that the x and y-dependent terms are never 90^0 out of phase. The phase shift is also not zero and depends exclusively on A and B, namely, is a function of the forcing parameters. Analogously to the case of longitudinal forcing, we have five distinct steady-state solutions.

Studying of (i)/(i*), (ii) and (iii)/(iii*) for different h, δ and σ makes it possible to establish the frequency domains where different types of resonant waves are stable. Theoretically, stability of each of these five solutions must be considered independently, but, of course, the dual solutions (ii) and (iii)/(iii*) have the same stability features. By assuming slow-time fluctuations of amplitudes $A, \bar{A}, B$ and $\bar{B}$, Faltinsen *et al.*Faltinsen et al. (2003); ? estimate effective frequency domains of stable steady-state regimes as $\delta \to 0$. The results are in satisfactory agreement with model tests. A particular conclusion is that, if $h \geq 0.4$, the steady-state solutions (ii) are either unstable or, having much larger energy, co-exist with (i). In practice, the fluid depths $h \geq 0.4$ disable 'squares'-like waves and, therefore, 'swirling' remains the sole common three-dimensional resonant wave for both types of excitations.

Another important finding consists of frequency domains where all of three steady-state wave regimes are unstable. Bearing in mind the possibility of chaos in those domains, we called them 'chaotic'. The dual steady-state solutions, first of all, 'swirling' render difficult identification of 'chaotic' domains from the experimental data, because switching between the dual solutions in transient phase ('swirling' changes direction of rotation) can deduce that we are in a 'chaotic' domain.

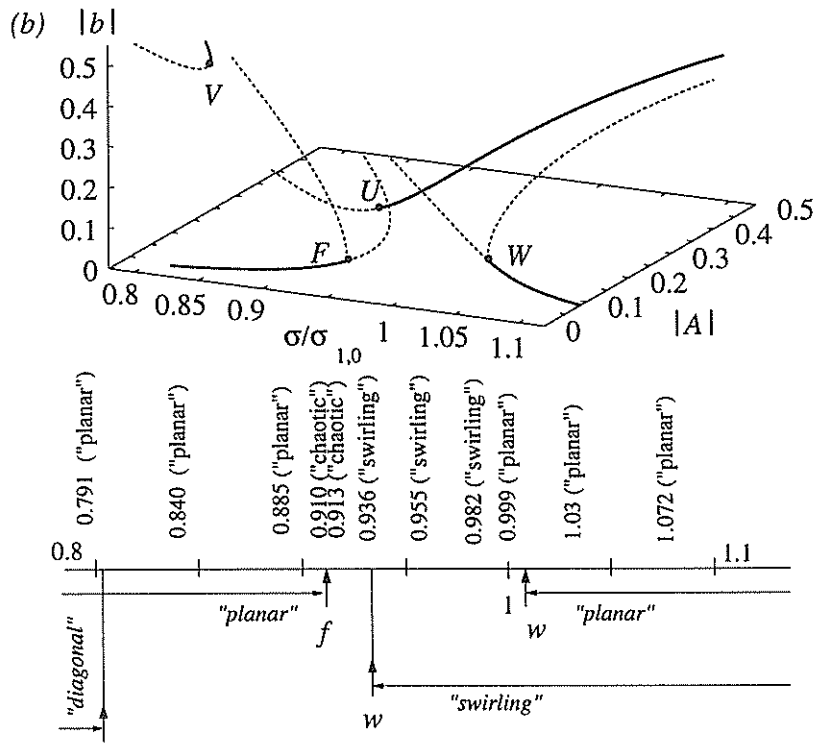

FIGURE 13. Typical wave response for square base and nearly-square base tanks.

Conclusions on 3D and questions: (to be formulated together with lecturer)

REFERENCES

Abramson, H.N.: 1966. The dynamics of liquids in moving containers. NASA Report, SP-106.

Abramson, H.N.: 1969. Slosh suppression. NASA Technical Report SP-8031.

Cariou, A. and G. Casella: 1999. Liquid sloshing in ship tanks: a comparative study of numerical simulation. *Marine Structures*, 12:183–198.

Chester, W.:1968 Resonant oscillation of water waves. I. Theory// Proc. R. Soc. of Lond., 306:5-22.

Chester, W., Bones, J.A.:1968 Resonant oscillation of water waves. II. Experiment// Proc. R. Soc. of Lond. 306:23-30.

Eastham, M.: 1962 An eigenvalue problem with parameter in boundary condition, *Quarterly Journal of Mathematics*, 13:112–140.

Faltinsen, O.M.: 1974 A nonlinear theory of sloshing in rectangular tanks. *J. Ship. Res.* **18**, 224–241.

Faltinsen, O.M., O.F. Rognebakke, I.A. Lukovsky, and A.N. Timokha: 2000 Multidimensional modal analysis of nonlinear sloshing in a rectangular tank with finite water depth, *Journal of Fluid Mechanics*, 407:201–234.

Faltinsen, O.M. and Timokha, A.N.: 2001 Adaptive multimodal approach to nonlinear sloshing in a rectangular rank. *J. Fluid Mech.* 432:167-200.

Faltinsen, O.M., Timokha, A.N.: 2002 Asymptotic modal approximation of nonlinear resonant sloshing in a rectangular tank with small fluid depth. J. Fluid Mech. 470:319-357.

Faltinsen, O.M., Rognebakke, O.F. and Timokha, A.N.: 2003 Resonant three-dimensional nonlinear sloshing in a square base basin. J. Fluid Mech. 487:1-42.

Hargneaves, R.: 1908 A pressure–integral as kinetic potential. Phil. Magazine, 16:436–444.

Ibrahim, R.A., Pilipchuk, V.N. and T. Ikeda: 2001. Recent advances in liquid sloshing dynamics, *Applied Mechanics Research*, 54(2):133–199.

Keulegan, G.H.: 1959 Energy dissipation in standing waves in rectangular basin. Journal of Fluid Mechanics, 6:33–50.

Lukovsky, I.A., Timokha, A.N.: 1995 Variational methods in nonlinear dynamics of a limited liquid volume. Kiev: Institute of Mathematics, 1995, 400pp. (in Russian).

Lukovsky, I.A., Timokha, A.N., 2002. Modal modeling of nonlinear fluid sloshing in tanks with non-vertical walls. Non-conformal mapping technique. *International Journal of Fluid Mechanics Research* 29(2): 216–242.

Whitham, G.B.: 1967 Variational methods and applications to water waves. Proc. Royal Soc. A299, # 1456:6–25.